Measurements of Acceleration Gap Dynamics in a 20-TW Applied-Magnetic-Field Ion Diode

J. E. Bailey, A. B. Filuk, A. L. Carlson, D. J. Johnson, P. Lake,
E. J. McGuire, T. A. Mehlhorn, T. D. Pointon, T. J. Renk, and W. A. Stygar
Sandia National Laboratories, Albuquerque, New Mexico 87185

Y. Maron
Weizmann Institute of Science, Rehovot, Israel 76100
(Received 3 October 1994)

The charged-particle dynamics in a 20-TW ion diode are determined from Stark-shift measurements of the accelerating electric field. The ~10-MV/cm peak field is an order of magnitude higher than any previous laboratory Stark-shift measurement. The data supply evidence for a field-limited ion source, a zero net-charge region near the anode, a positive net-charge region in the middle of the acceleration gap, and azimuthal asymmetries. Comparisons with QUICKSILVER computer simulations provide new capabilities to evaluate the influence of charged-particle dynamics on ion-beam divergence and power.

PACS numbers: 52.75.Pv, 32.60.+i, 52.25.Rv, 52.70.Ds

Pulsed-power applied-B ion diodes are a promising candidate driver for inertial confinement fusion (ICF) [1]. High-purity ~10-MeV lithium beams have been focused [2] to peak intensities of ~1.5-TW/cm^2 in a 10–15-nsec full width at half maximum (FWHM) pulse. However, significant diode improvements are needed to reach the 20–50-TW/cm^2 intensities required for high target gains. The two main issues presently limiting ion-beam power are beam divergence and the efficiency of converting electrical power into beam power. These issues are both strongly influenced by the charged-particle distributions in the acceleration gap.

This Letter describes time- and space-resolved measurements of the accelerating electric field profile and charged-particle distributions in an applied-B diode driven by the Particle Beam Fusion Accelerator II (PBFA II). Novel implementation of time-resolved spectrographs [3] results in a $\pm(2-5)\%$ electric field uncertainty. This is a factor of 4–10 lower than in previous work [4], despite the difficulties associated with operating at powers that are ~100 times higher. The peak electric field is ~10 MV/cm, an order of magnitude higher than any previous laboratory Stark-shift measurement. The field measured near the anode surface is 7–10 MV/cm, indicating that the current supplied by the LiF ion source is field limited rather than space-charge limited. The measurements provide evidence for new diode phenomena, including a region with zero net-charge density near the anode, localized positive net charge in the middle of the gap, and persistent azimuthal asymmetries. The results suggest improvements required in both experiments and simulations in order to accurately predict the power coupling efficiency and divergence.

The maximum diode ion current density in the absence of electrons is the Child-Langmuir space-charge limit $J_{CL} = k(Ze/m_i)^{1/2}V^{3/2}/d^2$, where Ze/m_i is the ion charge-to-mass ratio, V is the voltage, d is the physical acceleration gap, and k is a constant. The ion current can exceed this limit if electrons are introduced into the diode. However, efficient operation requires preventing the electrons from crossing to the anode. Applied-B diodes [5,6] use a magnetic field perpendicular to the accelerating electric field to insulate the anode-cathode (AK) gap against electron flow. A diagram of the cylindrically symmetric 15-cm radius PBFA II diode [6] is shown in Fig. 1. Conical magnetically insulated transmission lines (MITLs) connected to the top and bottom of the diode deliver a ~20-TW, 40-nsec FWHM power pulse. The 2–3-T magnetic field is applied by discharging a ~1-MJ capacitor bank through coils located in the anode and cathode. The strength of the magnetic field is adjusted so that the electron Larmor radius is less than the AK gap,

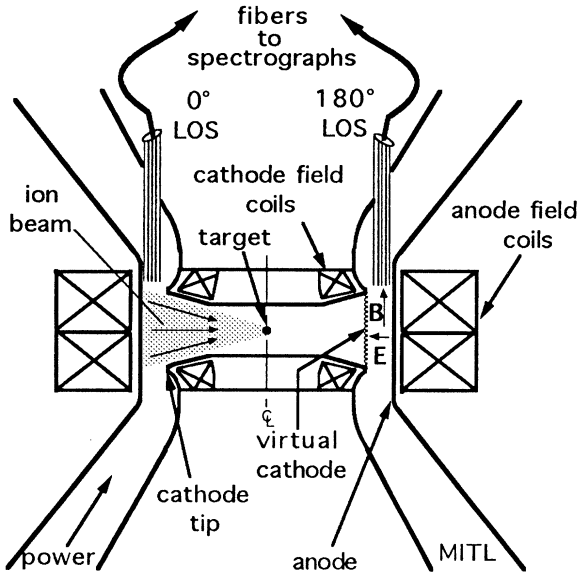

FIG. 1. Schematic of the PBFA II ion diode. The diode is cylindrically symmetric about the center line C_L and spectroscopic lines of sight (LOS) are located in two azimuths at 0° and 180°.

0031-9007/95/74(10)/1771(4)$06.00

but ions suffer only a small deflection. Electrons enter the diode either from the cathode tip plasma or by traveling along magnetic field lines that intersect the cathode side of the MITLs that deliver the power pulse. A virtual cathode, formed by electrons trapped on magnetic field lines at the cathode potential, enables extraction of the ion beam from the AK gap for transport to the ICF target. The ion current increases as electrons populate the region between the anode and virtual cathode, especially if the electrons move toward the anode via cross-field diffusion induced by nonuniformities or instabilities. The diamagnetism of the electron $\mathbf{E} \times \mathbf{B}$ drift (azimuthally in Fig. 1) may also move the virtual cathode toward the anode [7,8], shrinking the effective gap and further enhancing the ion current. The ion current density for a given ion species is thus determined by the voltage, the size of the dynamic gap between the anode and the virtual cathode, and the distribution of electrons in this gap.

The gap dynamics can also influence the ion-beam divergence. Electric fields perpendicular to the acceleration direction can be generated by either instabilities or nonuniformities in the charged-particle distribution. Computer simulations [9,10] and analytic modeling [11] predict that a rich variety of instabilities exist even in an idealized diode and potentially cause large beam divergence. The characteristics of the instabilities, and thus the induced divergence, depend strongly on the dynamic gap charged-particle distribution.

These considerations strongly motivate measurements of the charged-particle distributions. However, standard diagnostic techniques, such as interferometry or Stark broadening, are extremely difficult due to the combination of $\sim 10^{13}$-cm^{-3} particle densities and the pulsed high-power nature of the experiments. Most previous experiments [6] have attempted to infer the AK gap behavior from observations of the accelerated ion beam. One exception to this was the use of Stark-shift measurements by Maron *et al.* [4] to determine the electric field in a 0.1-TW, 1-MV ion diode. The measured dynamic gap size was approximately constant after an initial anode plasma expansion, and the electrons formed a diffuse cloud throughout the gap rather than a narrowly confined sheath. Other electric field distribution measurements are described in Refs. [12] and [13].

The PBFA II visible spectroscopy system. This uses lens-coupled fiber optics to collect light from ~2-mm-diameter, approximately cylindrical lines of sight parallel to the axis of symmetry and arranged radially across the AK gap. The fibers transport the light ~ 40 m to a remote screen room where time-resolved spectra are recorded with ~1-nsec resolution using streak cameras located in the exit focal plane of the spectrographs. Spectra from eleven spatial locations are measured in a single experiment with relative spacing accurate to ±0.2 mm and positioning accuracy relative to the anode surface of ±0.5 mm. The timing between spectra is accurate to ±0.4 nsec and the timing accuracy relative to the electrically recorded diagnostics is ±2 nsec.

The electric field is determined by measuring the Stark shift of LiI $2s$-$2p$ emission. This emission arises from lithium neutrals injected radially across the AK gap at velocities of ~50 cm/μsec when lithium ions accelerated from the LiF ion source undergo charge exchange in a thin (~10 μm) dense ($\sim 10^{18}$ cm^{-3}) contaminant layer. Although using emission from naturally occurring charge-exchange neutrals limits the midgap measurements to the time after neutrals travel from the anode across the gap, it has the important advantages that visible-light line intensities are higher than from ions and that the Doppler effects on the line profile are relatively small. We typically analyze lineouts from each spectrum at 15–20 sequential times, averaging over 4-nsec intervals to improve the signal-to-noise ratio. A single Gaussian is fit to each spectral line, with the wavelength uncertainty determined from the fluctuation level of the data about the fit using experimentally verified Gaussian statistics [14]. The shift is measured relative to the zero-field $2s$-$2p$ wavelength established using unshifted emission from after the power pulse. The typical 1σ uncertainty in the Stark shift is ±0.2–0.4 Å, compared to ~6-Å maximum shifts.

To ensure reliable results at 10-MV/cm fields, a previously unexplored regime for laboratory Stark-shift measurements, we used calculations of the Stark pattern performed independently at Sandia and at the Weizmann Institute [15]. Both calculations include Zeeman splitting, the effect of high-lying levels, and high-order terms in the expansion of the dipole matrix elements. The calculations agree to ~ 1% with available published data [16,17] that extend up to ~0.4 MV/cm. The difference between the two calculations is less than 10% over the range of fields encountered in these experiments. This uncertainty is not included in the error bars presented below.

The strategy we follow is to measure $|\mathbf{E}(x, \phi, t)|$ and determine the charged-particle densities from $\nabla \cdot \mathbf{E} = 4\pi\rho = 4\pi e(Zn_i - n_e)$, where x is the radial distance away from the anode, e is the electron charge, and Ze is the ion charge. The net-charge density ρ is determined by fitting a curve to the electric field data and differentiating with respect to x. We neglect any nonradial electric field components, consistent with estimates of the nonradial field based on preliminary experiments using spectroscopic lines of sight azimuthally separated by 2 mm. The ion velocity is given by $v_i^2(x) = (2\ Ze/m_i) \int_0^x E\, dx'$ and we determine the ion density from $n_i(x) = J_i/Zev_i(x)$, where J_i is the ion current density measured with dB/dt loops and Faraday cups. We assume that all ions originate at the anode surface with Ze/m_i equivalent to Li^{+1}. The electron density n_e is obtained by subtracting ρ from the ion density n_i.

A sequence of electric field profiles from a PBFA II experiment using a 6-cm-tall anode and an 18-mm-wide AK gap is shown in Fig. 2. Note that the 1σ error bars are often smaller than the symbol size. At the onset of ion current (t = 46 nsec) we typically observe a

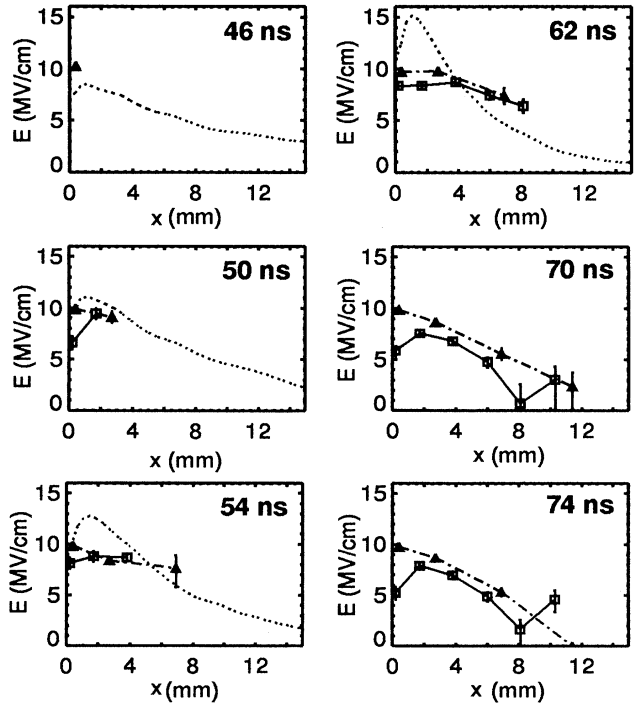

FIG. 2. Electric field evolution as a function of x, the radial distance away from the anode. The squares and triangles are measurements from a PBFA II experiment at the 180° and 0° azimuths, respectively. The dashed curve is a QUICKSILVER simulation result.

9–10-MV/cm electric field near the anode surface. The voltage at this time is ~10 MV, measured by analyzing ions Rutherford scattered from a thin foil with a magnetic spectrometer [18]. The corresponding average field in the absence of charged particles is ~5 MV/cm. The PBFA II field near the anode is almost twice as large, implying that electrons have already greatly modified the AK gap. This initially broad electron distribution must be incorporated into diode models.

The electric field measured at the anode surface is 7–10 MV/cm over most of the lithium-beam pulse, in contrast to the zero field expected for a space-charge-limited plasma ion source. This result is consistent with a recent theoretical hypothesis [19] that the LiF ion source produces Li ions via electron-assisted field desorption. At peak lithium-ion power (t = 62 nsec) dE/dx in the region between 1 and 6 mm from the anode is nearly zero. This implies that the net-charge density is about zero and $n_e \sim n_i$ in this region. The charged-particle densities derived from the 180° azimuth electric field data at t = 62 nsec are shown in Fig. 3. The PBFA II ion density is not shown in this plot, but it is about the same as the electron density. Note that the ion charge-to-mass ratio begins to change about 15 nsec after the ion current starts, when contaminant ions [2] other than Li^{+1} are accelerated. The impact of this change, estimated using the measurements described in Ref. [2], is that the true

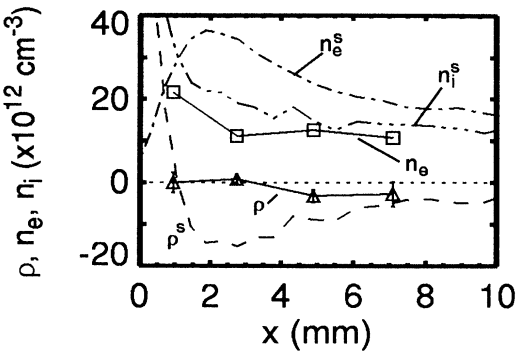

FIG. 3. Charged-particle distributions corresponding to the 180° azimuth at t = 62 nsec in Fig. 2. The curves marked with triangles and squares are PBFA II net-charge density and electron density, respectively. The dashed, triple-dot-dashed, and dot-dashed curves are simulation net charge, ion, and electron densities, respectively.

PBFA II ion and electron densities may be 30% lower than in Fig. 3. The electron density is roughly constant between 2 and 8 mm from the anode, but is ~2 times higher 1 mm from the anode. The rise in the derived electron density near the anode is contrary to expectations based on the simulations discussed below.

Azimuthal electric field nonuniformities of ±(10–20)% (Fig. 2) appear in every experiment to date. The persistence of the nonuniformities indicates that $\mathbf{E} \times \mathbf{B}$ azimuthally drifting electrons are unable to cancel them even though the drift time between the azimuthal locations is ~5 nsec. Nonuniformities perturb the orbits of azimuthally drifting electrons, increasing the diffusion rate across the magnetic field. Thus, they could contribute to the anomalously high electron density near the anode that is suggested by the observation that $dE/dx \sim 0$. Possible mechanisms contributing to the nonuniformities are electromagnetic fluctuations induced by instabilities, nonuniformities in the ion emission, and nonuniform injection of electrons from the MITL or cathode tip plasmas.

A strong perturbation in the midgap charged-particle distribution is observed just after peak ion power (Fig. 2, 70 and 74 nsec). The signature of this feature is a reversal in the sign of dE/dx from negative to positive, implying positive net charge due to either a localized deficit of electrons or surplus of ions. Although the uncertainty in the field is large enough to permit interpretation as merely a flattening of the field slope rather than sign reversal, repeated experiments show that the most probable values of the field exhibit the slope reversal. Further evidence that dE/dx reverses sign is provided by requiring that the integral of the field equals the voltage. The integral of the 0° azimuth data at 70 and 74 nsec is within ~0.5 MV of the measured voltage. This implies that the virtual cathode in this azimuth has probably moved ~5 mm from the cathode tip toward the anode. However, at the same times the integral of the field data from

the 180° azimuth is ~2.5 MV lower than the voltage. Extrapolating the field beyond the measurements with a monotonic decrease cannot account for this difference; the field must rise in the remaining portion of the gap. Mechanisms that might produce such an effect are under investigation. The above result also implies that the virtual cathode location in the 180° azimuth is several mm closer to the cathode than in the 0° azimuth. Work is in progress to determine whether this large unexpected azimuthal variation in the virtual cathode location is reproduced in other experiments.

The measurements enable detailed comparisons with three-dimensional (3D) electromagnetic particle-in-cell simulations using the QUICKSILVER computer code [10]. The code simulates a $\pi/8$ azimuthal section of the diode, including the 30-cm section of the MITL nearest the diode, using realistic geometry and accurate B-field topology. The input voltage to the MITL is adjusted to reproduce the experimental MITL voltage. The field-limited ion source is taken into account by using an 8-MV/cm threshold field for ion emission. With this limited set of input parameters, the code calculates the self-consistent, fluctuation-driven, 3D electron and ion dynamics from first principles.

QUICKSILVER simulation results are superimposed on the data in Figs. 2 and 3. As in the experiment, at ion current onset electrons fill the simulation gap, although the somewhat lower simulation electric field indicates that the simulation electron density is lower. The simulations suggest that this early population of electrons is due to injection from the MITL. The growth of the midgap electron density that accompanies the ion current growth is faster in the simulation, leading to higher calculated electric fields near the anode. The slower experimental electron density buildup is probably due to more rapid loss to the anode. However, the contaminant ion current is not presently included in the simulations and possibly contributes to the discrepancy. Unlike the experiments, where the electron density varies little in most of the gap and increases near the anode (i.e., $n_e \sim n_i$), the simulation electron density increases from 6 to 1.5 mm and decreases between 1.5 and 0 mm from the anode surface. The localized positive net charge in midgap and the azimuthal asymmetries are only observed in the experiment and not in the necessarily idealized simulations.

These measurements provide the first detailed experimental tests of our understanding of high-power ion diode acceleration gap physics. The simulation electric fields agree with the measurements to within ~15% during the first ~5 nsec of the ion beam. However, significant discrepancies arise later, implying that considerable improvements in both simulations and experiments are necessary before accurate predictions of diode behavior are possible. This is particularly important for calculations of instability induced beam divergence, since they rely on accurate knowledge of the time-dependent electron density distribution and the nonideal phenomena in the actual diode limit the present simulation fidelity. The results also suggest that diode efficiency and divergence would benefit from a reduction in the azimuthal nonuniformities.

We would like to thank the PBFA II operations crew and D. W. Wenger for technical asistance in fielding the experiments. We are also grateful to S. A. Slutz, T. R. Lockner, and M. P. Desjarlais for many useful discussions and to D. L. Cook, R. J. Leeper, and J. P. Quintenz for continuous support and encouragement. This work was supported by the U.S. Department of Energy under Contract No. DE-AC04-94AL85000.

[1] J. P. VanDevender and D. L. Cook, Science **232**, 801 (1986).
[2] T. A. Mehlhorn, in Proceedings of 10th International Conference on High Power Particle Beams, 1994 (to be published).
[3] J. Bailey, A. L. Carlson, R. L. Morrison, and Y. Maron, Rev. Sci. Instrum. **61**, 3075 (1990); J. E. Bailey, A. L. Carlson, and P. Lake, in Proceedings of the 1994 IEEE International Conference on Plasma Science, Santa Fe, 1994 (IEEE Report No. 94CH3465-2, 1994), p. 133.
[4] Y. Maron, M. D. Coleman, D. A. Hammer, and H. S. Peng, Phys. Rev. Lett. **57**, 699 (1986); Phys. Rev. A **36**, 2818 (1987).
[5] S. Humphries, Jr., Nucl. Fusion **20**, 1549 (1980).
[6] D. J. Johnson *et al.,* J. Appl. Phys. **53**, 4579 (1982).
[7] S. A. Slutz, D. B. Seidel, and R. S. Coats, J. Appl. Phys. **59**, 11 (1986).
[8] M. P. Desjarlais, Phys. Rev. Lett. **59**, 2295 (1987).
[9] M. P. Desjarlais *et al.,* Phys. Rev. Lett. **67**, 3094 (1991).
[10] T. D. Pointon *et al.,* Phys. Plasmas **1**, 429 (1994).
[11] S. A. Slutz and W. A. Johnson, Phys. Fluids **B4**, 1349 (1992).
[12] M. D. Coleman *et al.,* in Proceedings of the 12th International Conference on Plasma Physics and Controlled Nuclear Fusion Research, Nice, France, 1988 (Report No. IAEA-CN-50/B-4-1).
[13] B. A. Knyazev, S. V. Lebedev, and P. I. Melnikov, Zh. Tekh. Fiz. **61**, 6 (1991) [Sov. Phys. Tech. Phys. **36**, 250 (1991)].
[14] R. L. Coldwell and G. J. Bamford, *The Theory and Operation of Spectral Analysis Using ROBFIT* (AIP, New York, 1991).
[15] E. Stambulchik and Y. Maron, Weizmann Institute of Science Report No. WIS-90/40/Sept.-PH, 1994 (unpublished).
[16] L. R. Hunter, D. Krause, Jr., D. J. Berkeland, and M. G. Boshier, Phys. Rev. A **44**, 6140 (1991).
[17] L. Windholz, M. Musso, G. Zerza, and H. Jager, Phys. Rev. A **46**, 5812 (1992).
[18] R. J. Leeper *et al.,* Rev. Sci. Instrum. **59**, 1860 (1988).
[19] T. A. Green (private communication); R. W. Stinnett *et al.,* in Proceedings of the 9th International Conference on High Power Particle Beams, Washington, DC, 1992 (Report No. NTIS PB92-206168), p. 788.